The effect of different process configurations on the performance and cost of potassium taurate solvent absorption

Minh T. Ho[1*], Enrique Garcia-Calvo Conde[1], Stefania Moioli[2] and Dianne E. Wiley[1]

1.School of Chemical and Biomedical Engineering, The University of Sydney, Sydney Australia

2. *Dipartimento di Chimica, Materiali e Ingegneria Chimica "G. Natta", Politecnico di Milano, Piazza Leonardo da Vinci 32, I-20133 Milano, Italy*

Abstract

The main method of capture of CO_2 in industry is the use of solvents for CO_2 absorption in post-combustion capture and the benchmark solvent is monoethanolamine (MEA). However, it presents a few disadvantages such as having a high energy requirement while also being corrosive and toxic. Potassium taurate (K-Tau) is a solvent with the potential to replace MEA because it has similar reaction rates, high cyclic loading, degradation resistant and most importantly, low energy requirement.

The objective of this study was to compare and evaluate the effect of different process configurations on the reboiler duty for the precipitating potassium solvent absorption process. Utilising a baseline potassium taurate process, different process configurations were developed in Aspen Plus. These are a cold rich bypass (CRB) of the rich solvent stream to the stripper and a solid-liquid separator. The results show that the modified configurations reduce the reboiler duty of the potassium taurate process by approximately 12% through the reduction in sensible heat and vaporization duty.

Keywords: Potassium taurate, CO_2 capture, Stripper configurations

* Corresponding author. *minh.ho@sydney.edu.au*

1. Introduction

Traditionally, chemical absorption by amine solvent is used to remove acid gases (Kohl and Nielsen, 1997). Recently, alternative solvents have been investigated for possible application to CO_2 including amino acid solvents (Aronu et al., 2013, Lerche, 2012, Majchrowicz, 2014, Majchrowicz et al., 2009, Simons et al., 2010, Vaidya et al., 2010, van Holst et al., 2009). This class of solvent may be advantageous in comparison with traditional amines due to the solid precipitation, which, according to the Le Chatelier's principle, favours the absorption of carbon dioxide and therefore enhance the overall process. Among several types of amino acids that can be used, potassium taurate is one of the promising solvents.

Potassium taurate reacts with CO_2 (R1) to form a carbamate ion in solution and a zwitterion which precipitates as a result of its limited solubility.

$$\mathrm{CO_2} + \mathrm{K_2CO_3(aq)} + \mathrm{H_2O(aq)} \leftrightarrow 2\mathrm{KHCO_3(aq)} \quad \text{(R1)}$$

potassium carbonate — potassium bicarbonate

The process is described by two main reactions (Sanchez-Fernandez et al., 2014, Raksajati et al., 2016):

CO_2 absorption reaction:

$$\mathrm{CO_2} + 2^{-}\mathrm{OOC-R-NH_2(aq)} \leftrightarrow {}^{-}\mathrm{OOC-R-NH-COO^{-}(aq)} + {}^{-}\mathrm{OOC-R-NH_3^{+}(aq)} \quad \text{(R2)}$$

amine — Carbamate — Zwitterion

Protonated amine (zwitterion) precipitation:

$$^{-}\mathrm{OOC-R-NH_3^{+}(aq)} \leftrightarrow \mathrm{COOH-R-NH_2(s)} \quad \text{(R3)}$$

According to R2, most of the absorbed CO_2 takes the form of a carbamate ion. The CO_2 absorption reaction implies that for every molecule of absorbed CO_2, one carbamate ion and one zwitterion are formed (Brouwer et al., 2005).

Fundamental research on the use of potassium taurate as a solvent for the capture of CO_2 started with initial publications on studies to assess the equilibrium solubility of CO_2 in aqueous solutions of potassium taurate. In a series of experimental works, Kumar et al. (2003a) published the crystallisation characteristics of CO_2, the vapour-liquid equilibrium data (Kumar et al., 2003b) and the reaction kinetics of CO_2 and potassium taurate (Kumar et al., 2003c). Following research studies covered the investigation of the physical and thermodynamic properties of potassium taurate (Han et al., 2012, Aronu et al., 2013, Wei et al., 2013, Wei et al., 2014). Various publications extending the knowledge on the solubility (Wei et al., 2013, Wei et al., 2014, Sanchez-Fernandez et al., 2013b, Sanchez-Fernandez and Goetheer, 2011), absorption kinetics and reaction rates of potassium taurate in the presence of CO_2 (Aronu et al., 2013) were published in the following years .

The precipitating nature of potassium taurate requires various adaptations to the traditional absorber-stripper equipment design employed in non-precipitating systems (Brouwer et al., 2005). Therefore, employing process equipment capable of handling solid material contributes towards achieving the potential that precipitating systems present to reduce energy consumption and cost. In 2003, Versteeg et al. (2003) developed the first patented enhanced CO_2 absorption process intended to handle precipitating solids, which was later named DECAB (Versteeg et al., 2003, Feron, 2016).

1.1. Objectives

In this paper, the objective is to provide a preliminary assessment of the potassium taurate system for post-combustion capture, as well as to compare and evaluate the effect of different process configurations on the performance of the process.

2. Methodology

2.1. Case studies

The techno-economic modelling of this study has been limited to the recovery section of the CO_2 capture process, as represented in Figure 1. Analyses of the costs of the upstream flue gas scrubbing section and downstream CO_2 purification have not been included in the analysis. Similarly, transportation and storage of the captured CO_2 has not been included. CO_2 compression for transport is not included in the technical or general economic analysis in this study. However, to be consistent with previous studies, the final avoided capture costs and net energy penalty includes this component (CO_2 is compressed to 110 bar).

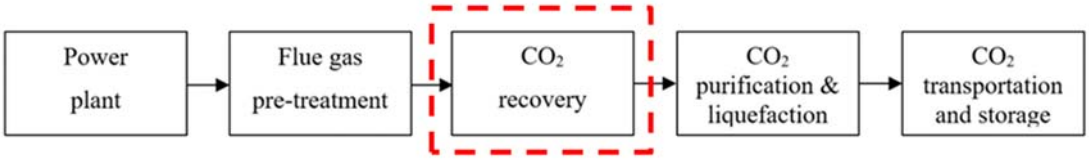

Figure 1 Boundary of the study; encompassing only the absorption, heat exchange and desorption

The case study used for the analysis focuses on post-combustion removal of CO_2 from a 500 MW coal-fired power plant. The wet flue gas entering the absorption process is assumed to be at a temperature of 313.15 K and a pressure of 1.01 bar, with a CO_2 composition of 13% mol, 5% mol O_2, 7% mol H_2O and 75% mol N_2. The flowrate of the wet flue gas is 19.6 kmols/s. It is assumed that the flue gas is free of any NO_x, SO_x and ash contents. The CO_2 recovery is assumed to be 90%. The CO_2 emission from the reference power plant is 0.88 t/MWh.

Detailed descriptions of the potassium taurate process can be found in (Moioli et al., 2017, Raksajati et al., 2016, Sanchez-Fernandez, 2013).

Utilising the baseline process simulation originally developed by Moioli et al. (Moioli et al., 2017) and shown in Figure 2, this study adapted the process for the following configurations:

Cold rich bypass (CRB) of the rich solvent stream to the stripper (

a) Figure 3)– the CO_2-rich solvent stream out of the split, with one stream heated in the cross heat exchanger while the other stream is not heated. The CRB split fraction into the stripper is also varied.
b) Addition of a solid-liquid separator (SLS) (Figure 4) – the CO_2 rich solvent stream passes through a hydrocyclone to create a solid rich slurry (underflow) and liquid stream (overflow). The underflow-to-total-flow split ratio (U/T) is set at 0.8 (Raksajati et al., 2016).
c) Combination of both the CRB and SLS configurations (Figure 5).

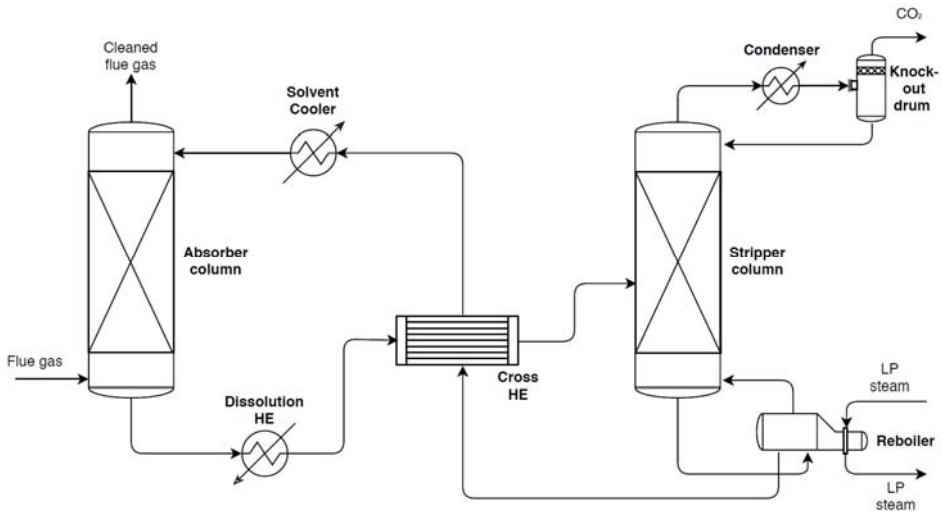

Figure 2 Process flow diagram of the Baseline potassium taurate process

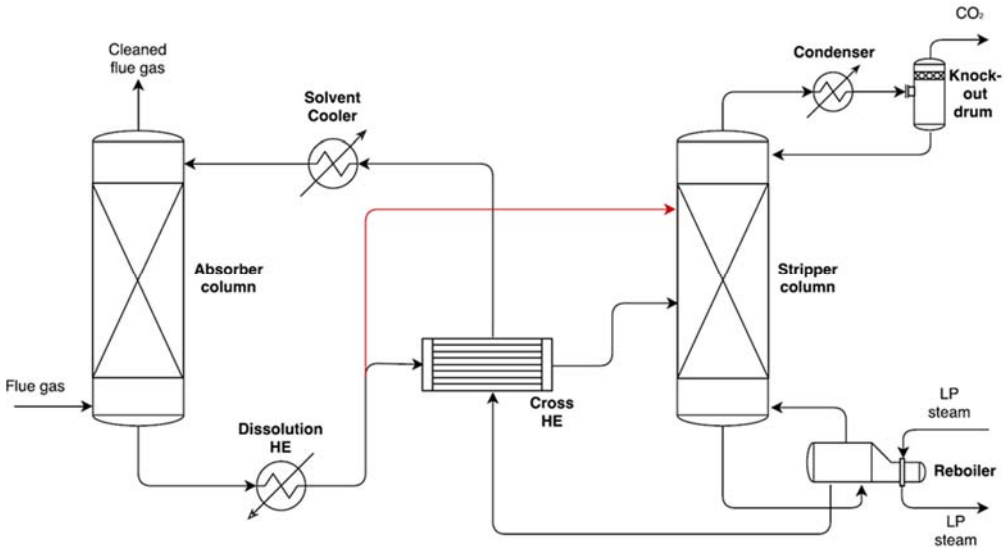

Figure 3 Process flow diagram for the cold rich bypass (CRB) configuration

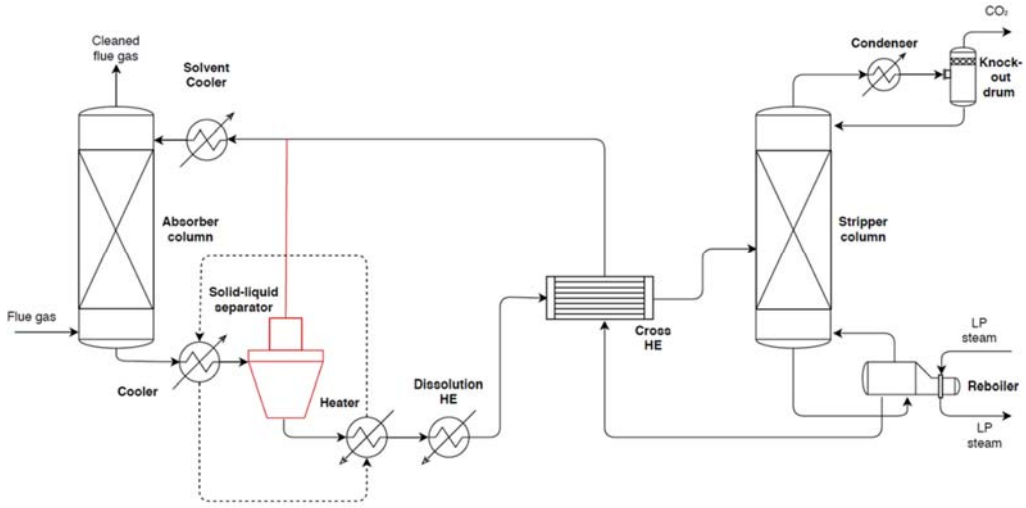

Figure 4 Process flow diagram for the hydrocyclone (solid-liquid separation, SLS) potassium taurate process

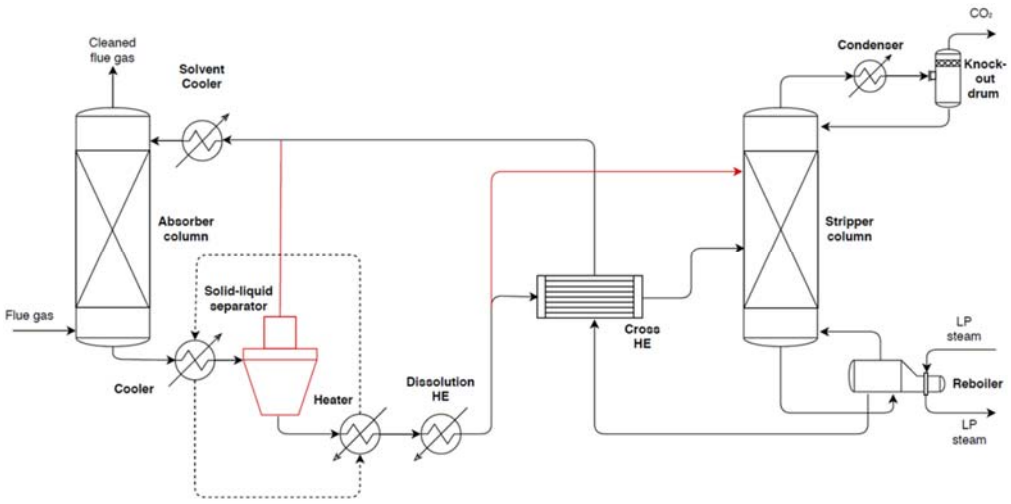

Figure 5 Process flow diagram of the combined CRB/SLS potassium taurate process

2.2. Process modelling

This study uses the model developed by Moioli et al. (2018) for the baseline analysis. Details outlining the development of the model can be found in (Moioli et al., 2017, Moioli et al., 2018). In this model all the electrolyte species not present by default in the Aspen software and the proper thermodynamics of the system have been taken into account. The absorber and stripper were both modelled with the RADFRAC column run in rate-based mode taking into account the mass and heat transfer resistances in ASPEN Plus®(AspenTech, 2014).

In the absorber, the unit is a RadFrac column assumed to operate adiabatically. The unit follows a non-equilibrium mass transfer rate-based calculation related to the direct and backward reactions for formation of carbamate and to the forward and backward reactions for formation of bicarbonate where the following set of reactions take place:

$$\mathrm{TAUH^+ + H_2O \leftrightarrow TAURINE + H_3O^+} \quad \text{(R4)}$$

$$\mathrm{2\,H_2O \leftrightarrow H_3O^+ + OH^-} \quad \text{(R5)}$$

$$\mathrm{HCO_3^- + H_2O \leftrightarrow CO_3^{2-} + H_3O^+} \quad \text{(R6)}$$

$$CO_2 + OH^- \rightarrow HCO_3^- \quad \text{(R7)}$$

$$HCO_3^- \rightarrow CO_2 + OH^- \quad \text{(R8)}$$

$$CO_2 + TAU^- + H_2O \rightarrow CARBAM^{2-} + H_3O^+ \quad \text{(R9)}$$

$$CARBAM^{2-} + H_3O^+ \rightarrow CO_2 + TAU^- + H_2O \quad \text{(R10)}$$

$$TAURINE + H_2O \leftrightarrow TAU^- + H_3O^+ \quad \text{(R11)}$$

120

121 As the precipitation reaction cannot be declared when the RADFRAC simulation is run in the rate-
122 based mode, the absorber unit cannot simulate the formation of solids. However, the effects which
123 the formation of a solid phase have on the process have been accounted for by (1) modifying the
124 chemical equilibrium data (2) adding a fictitious flash unit which estimates the amount of solid
125 taurine formed. The full details of this Aspen modelling approach have been detailed in Moioli et al.
126 (2018).

127 The stripper has been modelled as a RadFrac column composed of 20 stages, including the
128 condenser and reboiler, and using a non-equilibrium mass transfer rate-based calculation. The
129 stripper operates at a pressure of 1.8 bar. The CO_2 rich stream enters the desorption unit at the
130 second stage, while the released CO_2 and lean solvent leave at the top and at the bottom stages,
131 respectively. The reflux ratio selected for the condenser is 0.8, while the bottoms to feed ratio has
132 been specified to be 0.986, both specifications on a mole basis. The temperature of the stream
133 leaving the reboiler has been specified to be 120 ^oC, while the temperature at the top stage of the
134 unit has been specified to be 40 ^oC .

135 The cross heat exchanger has been set with a temperature difference of 10 ^oC and a minimum
136 temperature approach of 10 ^oC . The overall heat transfer coefficient remains constant at 850
137 W/m^2K.

138 .

139 Table 1 summarises the properties of absorber and stripper for the Baseline potassium taurate
140 process.

141 *Table 1 Properties of absorber and stripper for the K-Tau baseline process*

Properties	Absorber	Stripper
Inlet temperature of gas stream [°C]	40	-
Inlet temperature of solvent stream [°C]	40	108
Lean loading	0.27	-
Calculation type	Rate-Based	Rate-Based
Number of stages	20	20
Condenser	-	Partial Vapour
Reboiler	-	Kettle
Reboiler temperature [°C]	-	120
Pressure [bar]	1	1.8
Packing type	Mellapak Standard 250X	Mellapak Standard 250X
Section diameter [m]	20.7	16.6
Packing height [m]	20	17.6
CO_2 lean stream flowrate [kton/hr]	16.5	16.5

142

143 *2.3. Economic assumptions*

144 Table 2 summarises the key economic assumptions used in this paper. Further details about the
145 cost assumptions for cooling water, electricity and solvent can be found in Raksajati et al. (2016).
146 Costs for LP steam are plant specific as these are based on the efficiency penalty occurring when LP

147 steam is extracted from IEAGHG (2014). In this study, LP steam is assumed to be available at 3.5 bar
148 with no pressure drop between the extraction point and the reboiler. Estimation of the steam cost
149 has been extracted from NETL (2015).

150 *Table 2 Key economic assumptions*

Cost year	2016
Real yearly discount rate	7%
Plant lifetime	25 years
Construction year	40% completion in year 1 and remaining in year 2
Capacity factor	85%
Currency	USD
Water makeup	$1.8/kL
Cooling water	$0.345/GJ
Low pressure steam	$0.008/kg
Solvent	$3/kg
Electricity	$42/MWh

151 The capture plant is assumed to be an n^{th}-of-a-kind (NOAK) system. This assumption has a
152 considerable impact on the capture cost assumptions - such as contingencies - as NOAK systems
153 achieve cost reductions due to the experience gained, which reduces estimation uncertainty (Al
154 Juaied and Whitmore, 2009).

155 The overall capital cost has been estimated using Turton's Module Costing Technique (MCT) and
156 the methodology employed in CCS techno-economic reports by IEAGHG (Turton et al., 2008,
157 IEAGHG, 2014). The equipment costs estimated for the absorption process include the absorber,
158 stripper, reboiler, cross heat exchanger, coolers and condensers, pumps and blowers, dissolution
159 heater exchanger and hydro-cyclone (for the SLS case). General equipment such as storage facilities,
160 valves, secondary pumps were estimated as 30% of the sum of the cost of the total purchased

equipment. Table 3 summarises the breakdown in the capital cost calculations, where A, B1, B2, F_P and F_M are parameters for each item of equipment, with F_P depending on the pressure and F_M on the material of construction.

Table 3 Itemised cost factors

Capital cost element		**Sum of preceding items**
Purchase Equipment Cost (PEC)	A	
Bare Erected Cost	B	$B = f(A, B_1, B_2, F_P, F_M)$
Project Contingencies	C	10% of B
Process Contingencies	D	30% of B
Total Plant Cost	E	B+C+D
Inventory Capital	F	0.5% of E
Pre-production	G	2% of E
Owner's cost	H	7% of E
Total Capital Requirement	I	E+F+G+H

The operating costs include fixed costs such as maintenance, labour, administration and insurance. Variable operating costs comprise cooling water for the coolers, make up water for losses in the solvent cycle, solvent, electricity for pumps and steam cost for the reboiler (Table 2).

Cost of capture is calculated for both the amount of CO_2 captured and avoided:

$$\frac{\text{USD}}{\text{t CO}_2\text{captured}} = \frac{\text{NPV of project costs}}{\text{NPV of captured CO}_2} \quad \text{Eq. 1}$$

$$\frac{\text{USD}}{\text{t } CO_2\text{avoided}} = \frac{\text{NPV of project costs}}{\text{NPV of avoided } CO_2} \quad \text{Eq. 2}$$

171

3. Results and Discussion

3.1. Variations in the Cold Rich Bypass fraction

Figure 6 shows the reboiler and condenser duties with variations in the cold rich bypass split fraction into the stripper i.e. the fraction of the stream out of the absorber that bypasses the cross heat exchanger and is sent directly to the stripper. The cases shown are for where the cold bypass is fed into stage 2 and the CO_2 rich stream is fed into stage 10. The change in the split was investigated to see its interaction with the overall process and in particular, the reboiler duty. The split was varied from 1% to 15%. Figure 6 shows that the reboiler duty reduces as the amount of cold bypass increases from zero to 0.12, with the lowest reboiler duty and corresponding condenser duty becoming constant beyond 0.12. Using this split ratio, the stages at which the cold bypass and hot CO_2 rich stream are fed into the stripper is also varied (Figure 7). The analysis shows that the lowest reboiler duty occurred when the cold bypass is feed into stage 4, and the CO_2 rich stream is feed into stage 16. The subsequent results for the CRB and CRB-SLS cases are based on this scenario.

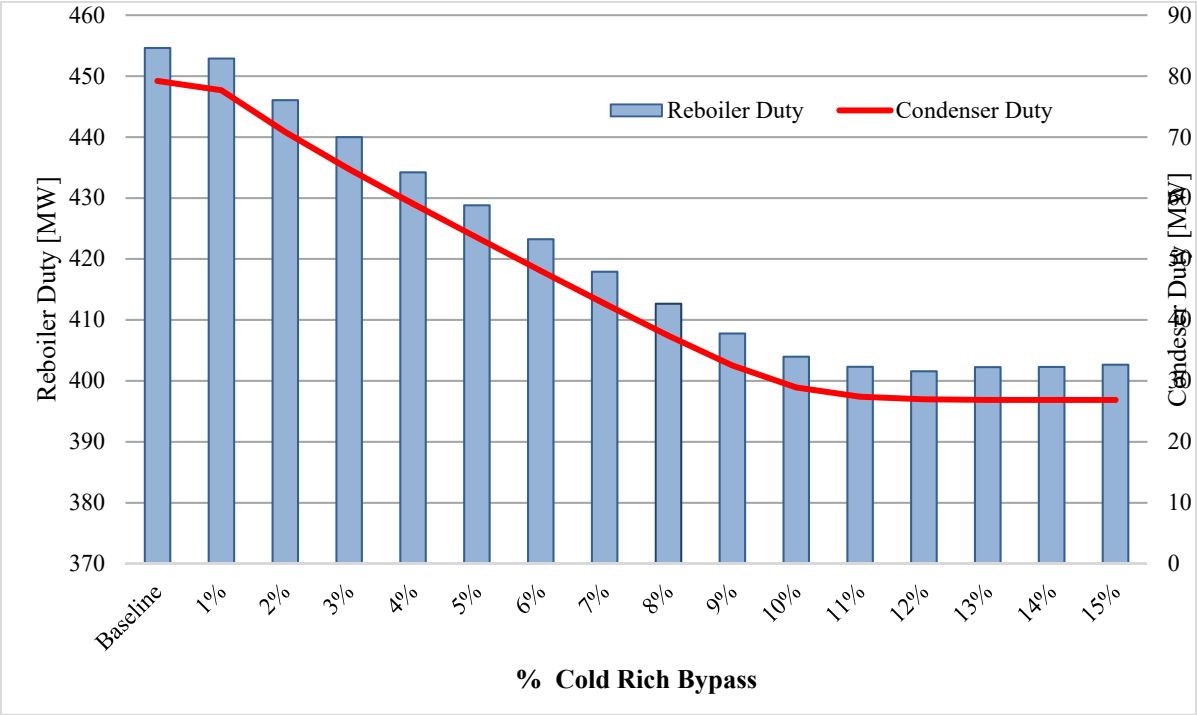

187

188 *Figure 6 Reboiler and condenser duties as a function of the percentage of the CRB split fraction selected*
189 *(cold bypass fed into stage 2, hot CO_2 rich stream fed into stage 10)*

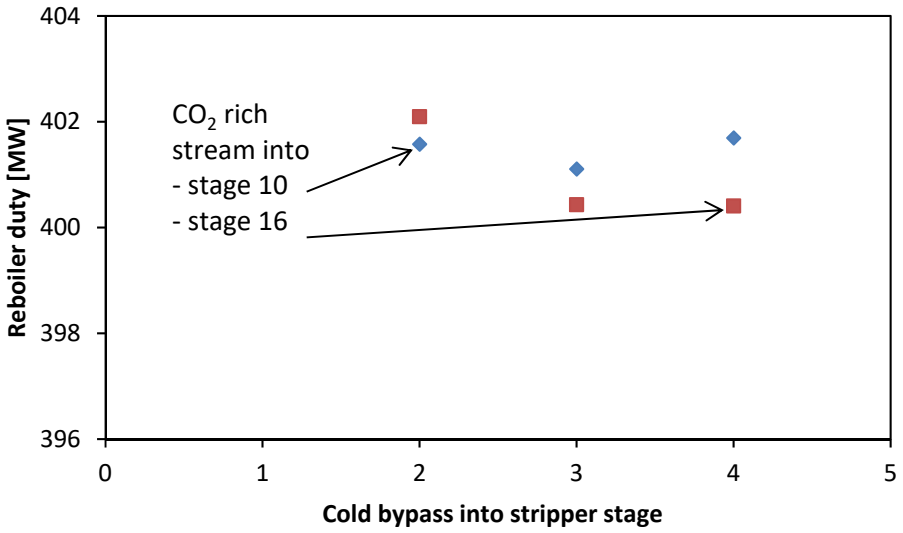

190

191 *Figure 7 Change in reboiler duty at different stages of the stripper at CRB of12%*

192

193 *3.2. Comparison of performance of different configurations*

194 *Table 4 Key technical outputs for three potassium taurate cases*

Process parameter	Baseline	CRB	SLS	CRB-SLS
Reboiler duty [MWth]	454	401	398	393
Total heat duty [GJ/t CO_2]	6.06	5.54	5.30	5.25
Reboiler duty [GJ/t CO_2]	4.50	3.97	3.94	3.89
Dissolution heat exchanger [GJ/t CO_2]	1.56	1.57	1.36	1.36
Condenser cooling duty [GJ/t CO_2]	0.78	0.25	0.86	0.24
Total cooler duty [GJ/t CO_2]	5.73	5.74	5.45	6.01
Cross heat exchanger duty [GJ/t CO_2]	5.20	5.22	5.65	5.08
Total pumping duty [MW/t CO_2]	1.03	1.04	1.16	1.16
Total energy penalty (excluding compression) [MWe]	115.3	105.5	101.2	100.3
Total energy penalty (including compression) [MWe]	149.3	139.5	135.2	134.3
Total energy penalty (%)	29.9%	27.9%	27.0%	26.9%
CO_2 rich solvent flowrate out of absorber [kton/hr]	16.8	16.8	20.3	20.3
Solvent working capacity [mol CO_2/mol solvent]	0.16	0.16	0.12	0.12
CO_2 rich loading [mol CO_2/mol solvent]	0.43	0.43	0.42	0.42
Temperature of rich solvent at stripper inlet [^oC]	108	111	110	110
Temperature at top of the absorber [^oC]	56.7	56.7	51.9	52.9
Boil-up rate (kgmols/s of water)	3.56	3.11	3.10	3.06

Table 4 summaries the key technical outputs for the three potassium taurate cases evaluated. The results show that the Baseline case study has the highest total heat duty, with 75% of the total heat duty attributable to the reboiler, while the remaining comes from the dissolution heat exchanger. In the CRB case, the reboiler and thus total heat duty reduce by about 12% from the Baseline decreasing from 4.5 GJ/t CO_2 to 3.97 GJ/t CO_2. According to Eisenberg and Johnson (1979), the split configuration maximizes the recovery of heat from the heat lean solvent. This is because a cold bypass configuration means that a smaller rich stream flowrate enters the cross heat exchanger (which can also be heated to higher output temperature) resulting in a lower sensible heat duty. Also, in the CRB case, the reboiler duty reduces because of reductions in the vaporisation duty as shown by the boil-up rate decreasing from 3.56 to 3.11 kmols/s. A significant reduction is also observed for the condenser duty in this case, decreasing from 0.78 GJ/t CO_2 to 0.25 GJ/t CO_2. This arises because introduction of the cold bypass into the top of the stripper reduces the temperature of the vapour fraction at the top stage and the corresponding work required by the condenser (Figure 8). The cold bypass acts as a cooling source, condensing some of the rising stripping steam and thus aiding the condenser. An additional benefit of using a CRB is the enhanced desorption of CO_2 observed for the top part of the column. This is shown in Figure 9, which presents the K-values for CO_2. The K-values, represent the vapor-liquid phase equilibrium values at the stage interface. The desorption of CO_2 is substantially enhanced in the upper stages of the stripper due to the drop in temperatures. The results suggest that the top section of the stripper is operating at much higher desorption efficiencies than the other lower stages.

215

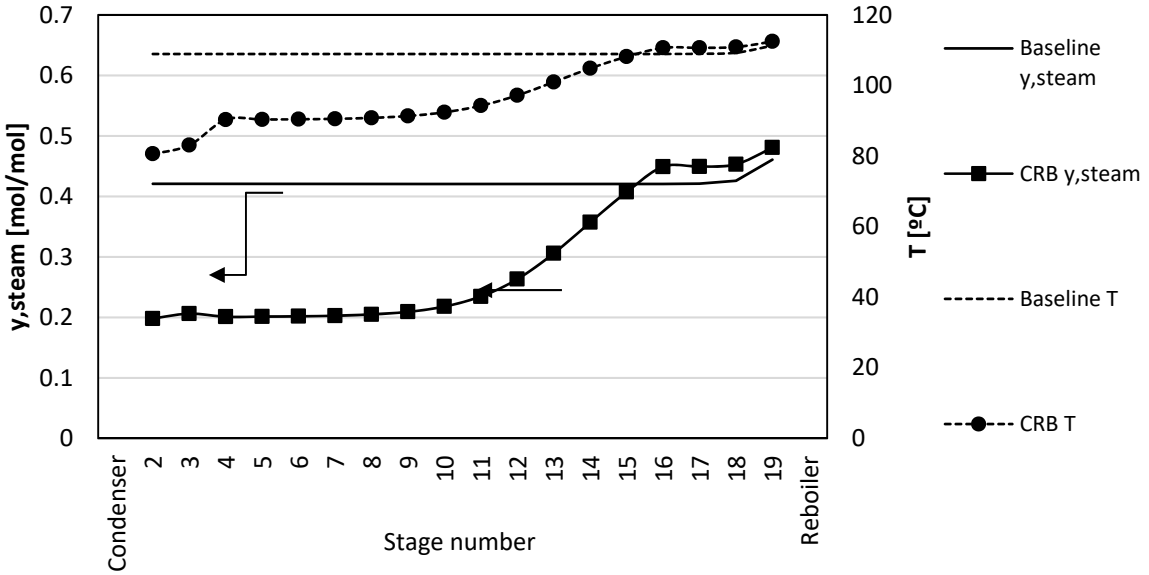

216 *Figure 8 Steam composition and temperature profiles in the stripper*

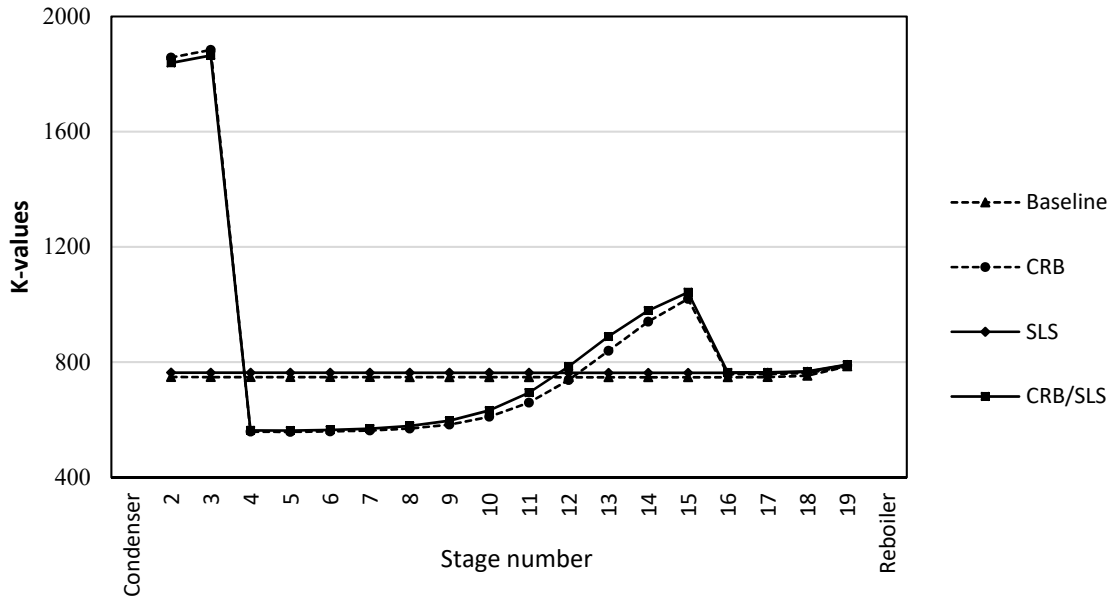

217

218 *Figure 9 Vapor-liquid K-values for CO_2 in each stage of the stripper*

For the SLS case, the total heat duty is less than both the Baseline and CRB cases, with lower duties arising in the dissolution heat exchanger and reboiler. This is caused by the interactions between the pH of the system and the partial pressure of CO_2, which is the driving force of the desorption process. When the CO_2 rich stream is sent to the hydrocyclone unit, the supernatant, which is basic as it is rich in potassium counter-ions, is separated from the slurry. The removal reduces the concentration of the potassium ions and, as a result, the pH of the system also decreases. As outlined in Sanchez-Fernandez et al. (2013a), a lower pH in the stripper feed translates to a higher partial pressure of CO_2, facilitating the CO_2 desorption resulting in lower heat of absorption and water vaporization duty. Although a reduction in reboiler duty is observed for the SLS compared to the Baseline, there is no real difference when compared to the CRB case. This is because in the SLS case, due to the presence of the hydrocyclone, the flowrate of the CO_2 rich slurry stream is much larger. In splitting the CO_2 rich stream, the lean loading of the solvent stream into the absorber increases from 0.27 to 0.3 mol CO_2/mol solvent. This is because some of the overflow from the solid-liquid separator is returned directly to the absorber without being regenerated. As a consequence, the working capacity reduces from 0.16 mol CO_2/mol solvent to 0.12 mol CO_2/mol. To achieve the fixed recovery rate of 90% CO_2, without increasing the size of the absorber, a much larger solvent flowrate is required. Although the lower pH from the slurry stream reduces the absorption and vaporization duty for this scenario, the larger solvent stream flow rate offsets any benefits. The results also show that for the SLS case, there is no reduction in the condenser duty compared to the Baseline case.

In the CRB-SLS configuration, in combining the effects of the previous two configurations, it is expected that the additive effects should result in a configuration with the lowest reboiler duty. The results show a reduction of 14% relative to the Baseline case, and 1.5% relative to the CRB and SLS cases. The lower reboiler duty arises from the reduction in the sensible heat component of the regeneration energy (because the inlet streams to the stripper are 2ºC hotter than in the Baseline case) together with the lower vaporization duty. Additionally, the heat duties of the condenser, cross-heat exchanger and dissolution heat exchanger for this configuration are also the lowest of all

246 cases. The heat duty reductions achieved for the dissolution heat exchanger and cross heat
247 exchanger observed in the CRB-SLS configuration occur due to the supernatant recycle and are the
248 same as those for the SLS case. Similarly, the reduction in the condenser duty is driven by the same
249 enhanced condensation and lower boil-up effects as observed in the CRB case.

250 Figure 10 and Figure 11 show the temperature profile and steam mass flowrate in the stripper for
251 the four configurations respectively. The figures show that temperature profile of the CRB and CRB-
252 SLS cases varies significantly along the stripper and are largely determined by the cooling effect of
253 the cold rich bypass, where lower temperatures are obtained for three fourths of the stripper
254 column. The results suggest that the operation of the stripper and its process variables are closely
255 dictated by the use of a CRB which influences the reduction in the vaporisation duty, while the use
256 of the hydrocyclone primarily impacts the sensible heat.

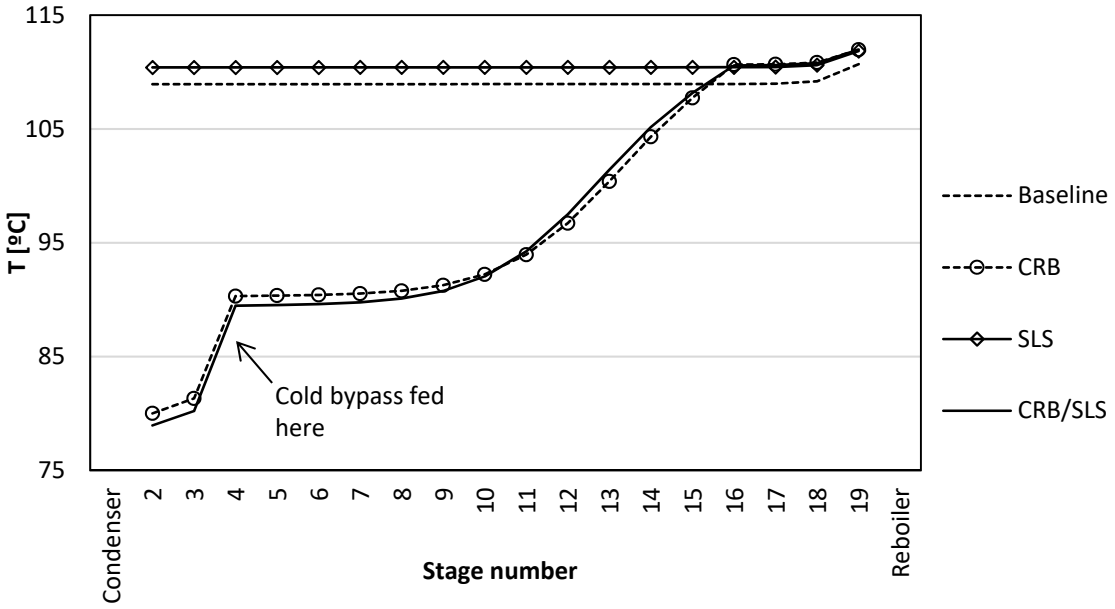

257

258 *Figure 10 Temperature profile of the liquid phase in the stripper for the four configurations*

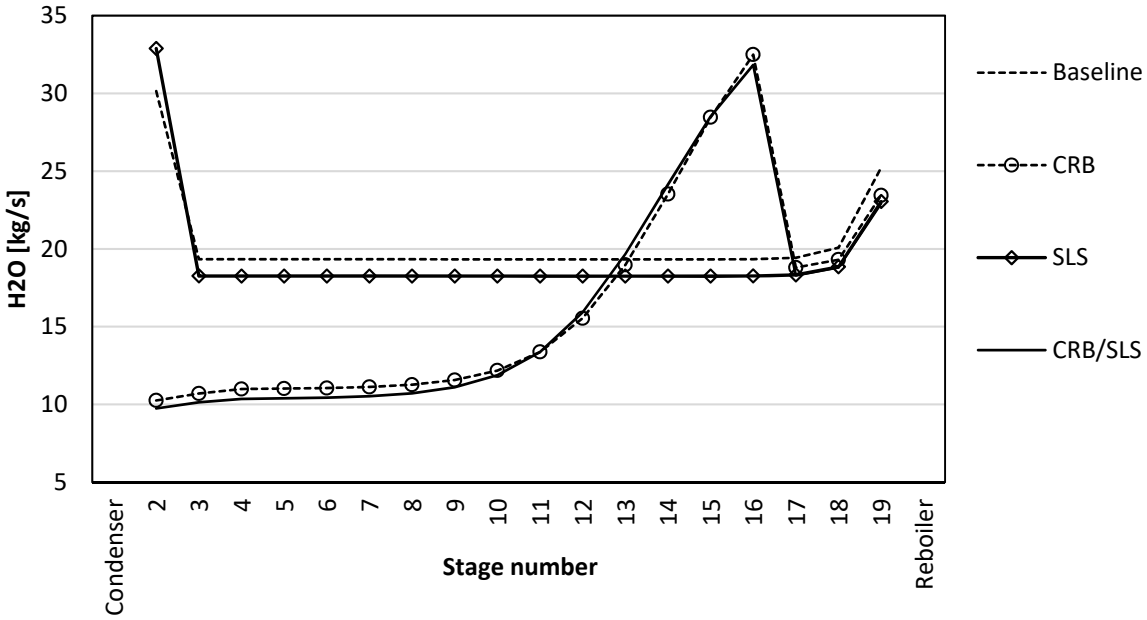

Figure 11 Steam mass flowrate profile for each of the four configurations

3.3. Economic evaluation

The capture costs for the different process configurations are summarized in Table 5 and Figure 12. The amount of CO_2 avoided and avoided cost presented in Table 5 includes the costs and energy consumption for CO_2 compression to 110 bar.

271 *Table 5 Summary of economic results for potassium taurate absorption process*

Economic parameter	**Baseline**	**CRB**	**SLS**	**CRB-SLS**
Total capital cost for absorption process only [$/kW (Net power)]	$1,308	$1,273	$1,455	$1,407
Total capital cost for absorption + compression [$/kW (Net power)]	$1,430	$1,392	$1,573	$1,524
Total operating cost for the absorption process [$/kWh]	$32	$29	$29	$28
Total operating cost for the absorption process + compression [$/kWh]	$37	$34	$34	$33
CO_2 avoided for absorption + compression [million t/yr]	1.78	1.84	1.87	1.88
Energy penalty [MWe]	149.5	139.5	135.2	134.3
$/t CO_2 avoided (without compression)	61.5	56.9	58.6	57.3
$/t CO_2 avoided (with CO_2 compression)	76.4	70.9	72.8	71.3

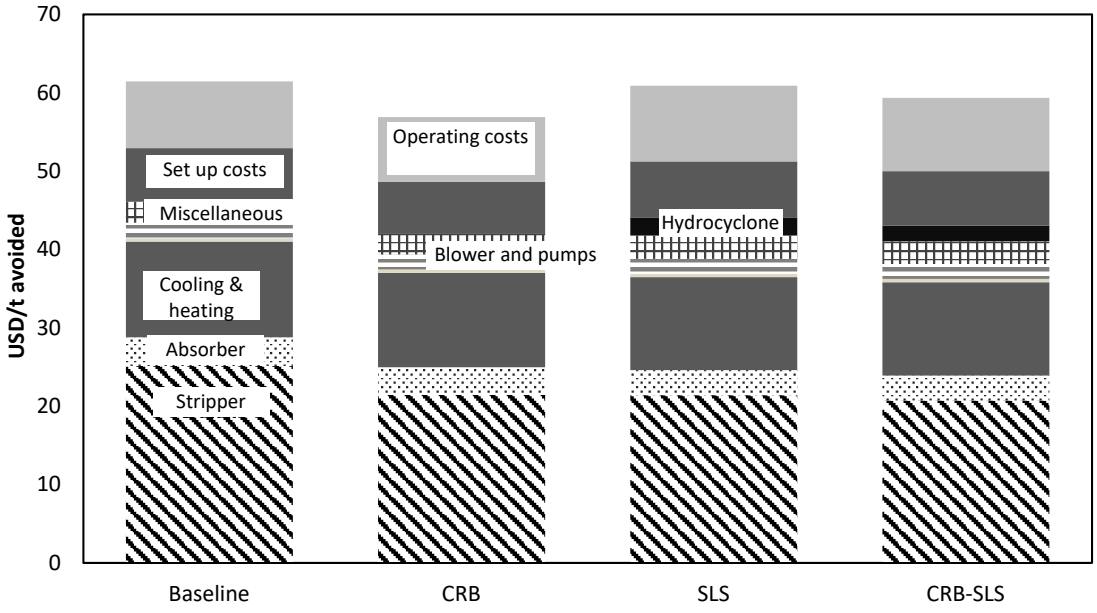

272

273 *Figure 12 Cost breakdown of the four potassium taurate configurations*

274

The economic results show that the configuration with the lowest cost is the CRB. This configuration has costs 5% lower than the Baseline because of the lower energy penalty and subsequent higher CO_2 avoided. Although the SLS and CRB-SLC configurations have lower energy penalties and higher CO_2 avoided than the CRB configuration, their overall avoided costs are higher. This is because for these cases, higher total capital costs offset any cost benefits of the reduced energy penalties and lower operating costs. The higher capital costs arise due to additional equipment such as the hydrocyclone and the larger cross-heat exchanger needed from the larger solvent flowrate. The economic results also suggest that although the CRB-SLS configuration results in better performance compared to the Baseline, economically it is not competitive.

Table 6 presents the change in capital cost for the three process modifications in greater detail, relative to the Baseline case. The results show that for all three configurations, the capital cost of the cross heat exchanger is much higher than in the Baseline, and is particularly so for the SLS case. The increase occurs because the cross heat exchanger unit for these cases requires a much larger surface area relative to the Baseline case. The increase in area needed is the result of the reduction of the temperature driving force of the streams entering the unit. This reduction is substantial in the SLS case, where the cross heat exchanger is 50% larger, with the increase in the heat transfer area requirements caused by the larger solvent flowrates (Table 4). For the CRB case, this increase is 12% and is needed to compensate for the lower flowrate in the cold side.

The largest capital cost reductions occur for the condenser and reboiler for the CRB and CRB/SLS cases, however the reverse is true for the SLS where an increase in capital cost relative to the Baseline case is observed. An important feature of the stripper inlet temperature is how it affects the reboiler and condenser duties. The hotter the inlet, the less sensible heat must be provided by the reboiler. However, hotter inlet temperatures lead to higher stripping steam vaporisation rates, which lead to an increase in the condenser duty. This occurs because the stripping steam cannot benefit as much for condensation from a hotter (compared to the baseline case) down-flowing solvent. This is exemplified in the case of the SLS, where the reboiler and condenser are markedly affected in opposite directions. While the reboiler duty is decreased by 14%, the condenser duty is

increased by 9%. This trade-off of duties is unique to the SLS case, as the enhanced condensation of the cases with a CRB negates any vaporisation due to higher temperatures into the stripper while simultaneously leading to lower reboiler duties. The opposite effect in the duties in the SLS case is one instance where hotter temperatures for the CO_2 rich stream into the stripper are desired, as the economic results suggest that it is reductions in the LP steam what should be sought, even if this leads to increased cooling water consumption in the condenser.

Minor capital cost reductions for the alternate configurations relative to the Baseline case are also observed for the dissolution heat exchanger, coolers, and pumps; primarily resulting from lower solvent flowrates passing through these units.

Table 6 Changes in the capital cost for the three configuration relative to the Baseline.

CAPEX				
Process block	Unit	Percentage change relative to Baseline		
		CRB	**SLS**	**CRB/SLS**
Heating and cooling	Cross heat exchanger	12%	29%	7%
	Dissolution heat exchanger	-	-8%	-8%
	Cooler	-	-4%	2%
Stripper	Condenser	-49%	22%	-51%
	Reboiler	-7%	-8%	-8%
Pumps	CO_2 rich stream pump	-	4%	4%
	CO_2 lean stream pump	-	-10%	-11%
Total CAPEX		**-**	**15%**	**12%**

Table 7 shows the change in operating cost for the three process modifications, relative to the

Baseline case. The analysis shows that the main reductions in operating costs for the CRB, SLS and CRB-SLS cases generally occur because less cooling water is needed in the coolers and condenser, and less steam is required for solvent regeneration in the reboiler. Overall, the operating costs are about 6% to 8% lower than the Baseline, or $3-4/kWh lower.

Table 7 Changes in the operating cost for the three configuration relative to the Baseline

OPEX					
Process block	Unit	Consumable	Percentage change		
			CRB	SLS	CRB/SLS
Absorber	Absorber vessel	Water makeup	-	-50%	-50%
Heating and cooling	Dissolution heat exchanger	LP steam	2 %	-13%	-12%
	Cooler	Cooling water	18%	-5%	5%
Stripper	Condenser	Cooling water	-62%	9%	-70%
	Reboiler	LP steam	-12%	-13%	-14%
Pumps	CO_2 rich stream pump	Electricity	-	4%	4%
	CO_2 lean stream pump	Electricity	-	-9%	-9%
Fixed operating costs			**-**	14%	11%
Total OPEX			**-6%**	**-6%**	**-8%**

3.4. Comparison with MEA

Compared to an absorption process using MEA solvent, the energy penalty of the baseline potassium taurate system at 29% is similar to that of a non-optimised MEA process of 27% (Li et al., 2016). As with the MEA process, the largest component of the energy usage in the potassim taurate system is the reboiler (accounting for 75% of the total energy penalty) and the CO_2 compressor (at

23% of the total), while for the MEA process the breakdown is about 58% and 30% respectively (Li et al., 2016). In the literature, typical costs for MEA solvent CO_2 avoided range from US$62.0 to US$95.2/tonne CO_2 (Li et al., 2016, NETL, 2015, NETL, 2010, Raynal et al., 2011); with the wide range in values being due to different capital cost methodologies, process boundaries and economic assumptions. Using the same economic assumptions as this study, the estimated cost for the baseline MEA process from the study by Li et al (2016) is $72/t CO_2 avoided, which is slightly cheaper than the estimated costs for the potassium taurate system in this paper. This difference arises because of the smaller reboiler duty (4 GJ/t of CO_2) and solvent flowrate for the MEA system. With regards to the capital cost estimates, for the potassium absorption processes these range from $1,308/kW for the baseline to $1,455/kW for the SLS case. Similar values for capital cost of $1,357/kW have been obtained for a baseline (non-optimised) MEA (Li et al., 2016).

However, the contribution of different process blocks to the total cost is significantly different for the two absorption processes. As shown in **Errore. L'origine riferimento non è stata trovata.**, the largest differences are in the compressor, stripper, heating and cooling process blocks.

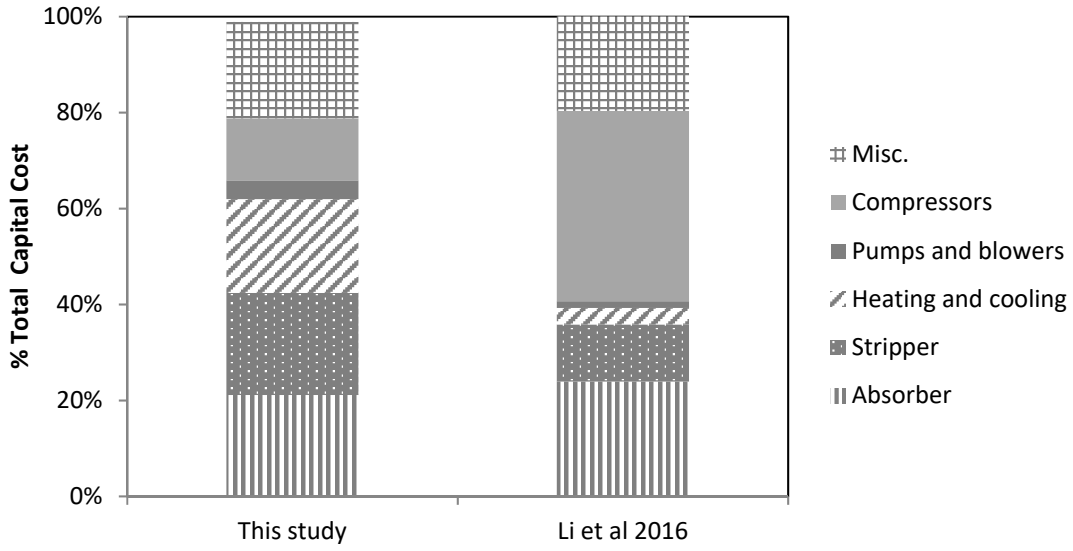

Figure 13 Breakdown in costs for the baseline KTau capture costs and an MEA process

For the MEA process (based on the breakdown in capital cost as detailed in Li et al. (2016), the largest cost component is for the compressor which comprises 40% of the total equipment bare erected cost (BEC). In this study, the compression makes up less than 15%. In contrast, the stripper contributions and heating and cooling blocks are much larger for the potassium taurate system. In this study, a very large solvent flowrate is required due to the small working capacity of the solvent (0.12 mol CO_2/mol solvent), which results in very large and more expensive cross heat exchangers being needed. The stripper for the potassium taurate system is also higher and wider at 17.6m x 16.6m compared to 7m x 9.5m for the MEA system in Li et al. 2016. In terms of the cost breakdown, the main difference between the two absorption processes lie in the heating and cooling block. In the MEA process, this system accounts for about 4% of the total capture cost, while in the potassium taurate process it accounts for 10%. The larger cost component arises because the lower capacity of the potassium taurate solvent, which is 0.10 mol CO_2/mol solvent smaller than that of MEA, leads to a larger solvent flowrate being required. A very large cross heat exchanger is also required, resulting in high costs both in absolute terms and on a per tonne of CO_2 avoided basis.

The costs estimates presented in this paper for the potassium taurate system are indicative Nth-of-a-kind values with a 30% error margin. Such Nth-of-a-kind costs will be significantly lower than first-of-kind plant costs because technology learning will significantly reduce the capital and operating cost. Furthermore, it should be noted that all costs contain uncertainties due to changes in factors such as exchange rate, fuel costs and labour rates. As a consequence of these uncertainties, if capital costs for the baseline potassium taurate system is 20 % higher than the estimate, the capture cost for the process would likely increase by six percent or \$4/t CO_2 avoided. Similarly, if the operating costs varied by 20%, through higher fuel or steam cost, the capture cost for the baseline process would increase by almost 15% or \$11/t CO_2 avoided.

4. Conclusion

This paper presents an evaluation of the performance and cost of three alternate process

configurations for post-combustion absorption using a precipitating potassium taurate solvent. The Baseline configuration was modified to include a cold-rich-bypass and/or solid-liquid-separator. By implementing these process changes, the regeneration duty for the process reduces by approximately 12% to 14%, with the flow on effect of lowering operating costs. While a solid-liquid-separator is beneficial for performance, if no changes to the absorber are undertaken, then the increase in capital costs due to the addition of the hydro-cyclone offsets any cost reductions from lower regeneration duties. The configuration resulting in the lowest capture cost was the cold-rich-bypass, as lower operating costs were realized without the compromise of higher capital costs.

In evaluating the different ratios of cold-rich-bypass fraction into the stripper, it was found that a split of 0.12 of the cold CO_2 rich solvent being sent to the stripper resulted in the lowest reboiler and condenser duties. Further increases in the split ratios were found to make no further improvements in the performance.

The techno-economic analysis of the different process configurations for potassium taurate absorption presented this paper provides a high level assessment highlighting areas of possible performance improvements and cost reductions. In this study, the working capacity and the corresponding solvent flowrates were not optimized. Further studies optimizing the absorber and stripper designs, coupled with investigating heat integration opportunities for these configurations would be worthwhile. Additional experimental studies to obtain more detailed data of fundamental solvent characteristics for the process simulation would also be valuable, as well as investigating the impact of alternate configurations such as absorber inter-cooling on the absorption and precipitation process.

5. References

Al Juaied, M. & Whitmore, A. 2009. Realistic costs of carbon capture. Energy Technology Innovation Policy Research Group, Belfer Center for Science and International Affairs, Harvard Kennedy School of Government, Harvard University, Cambridge, MA (United States)

Aronu, U. E., Ciftja, A. F., Kim, I. & Hartono, A. 2013. Understanding Precipitation in Amino Acid Salt systems at Process Conditions. *Energy Procedia,* 37**,** 233-240.

Aspentech 2014. *ASPEN Plus® Guidelines,* Burlington, MA, AspenTech.

Brouwer, J., Feron, P. & Ten Asbroek, N. Amino-acid salts for CO2 capture from flue gases. Fourth annual conference on carbon capture & sequestration, 2005.

Eisenberg, B. & Johnson, R. R. 1979. *Amine regeneration process*. Patent No. US 4152217 A1.

Feron, P. 2016. *Absorption-Based Post-Combustion Capture of Carbon Dioxide*, Woodhead Publishing.

Han, X.-W., Zhou, C.-R. & Shi, X.-H. 2012. Determination of specific heat capacity and standard molar combustion enthalpy of taurine by DSC. *Journal of thermal analysis and calorimetry,* 109**,** 441-446.

Ieaghg 2014. Techno Economic evaluation of different Post Combustion CO2 Capture Process Flow Sheet Modifications. *2014/08.*

Kohl, A. L. & Nielsen, R. 1997. *Gas Purification,* Houston, Texas, USA, Gulf Publishing Company, Book Division.

Kumar, P., Hogendoorn, J., Feron, P. & Versteeg, G. 2003a. Equilibrium solubility of CO2 in aqueous potassium taurate solutions: Part 1. Crystallization in carbon dioxide loaded aqueous salt solutions of amino acids. *Industrial & engineering chemistry research,* 42**,** 2832-2840.

Kumar, P., Hogendoorn, J., Timmer, S., Feron, P. & Versteeg, G. 2003b. Equilibrium solubility of CO2 in aqueous potassium taurate solutions: Part 2. Experimental VLE data and model. *Industrial & engineering chemistry research,* 42**,** 2841-2852.

Kumar, P., Hogendoorn, J., Versteeg, G. & Feron, P. 2003c. Kinetics of the reaction of CO2 with aqueous potassium salt of taurine and glycine. *AIChE Journal,* 49**,** 203-213.

Lerche, B. M. 2012. *CO_2 Capture from Flue gas using Amino acid salt solutions.* PhD Thesis, Technical University of Denmark.

Li, K., Leigh, W., Feron, P., Yu, H. & Tade, M. 2016. Systematic study of aqueous monoethanolamine (MEA)-based CO2 capture process: Techno-economic assessment of the MEA process and its improvements. *Applied Energy,* 165**,** 648-659.

Majchrowicz, M. E. 2014. *Amino Acid Salt Solutions for Carbon Dioxide Capture.* Master Thesis, University of Twente.

Majchrowicz, M. E., Brilman, D. W. F. W. & Groeneved, M. J. 2009. Precipitation regime for selected amino acid salts for CO_2 capture from flue gases. *Energy Procedia***,** 979-984.

Moioli, S., Ho, M. T. & Wiley, D. E. 2017. Simulation of CO_2 Removal by Potassium Taurate Solution. *Chemical Engineering Transactions,* 57**,** 1213-1218.

Moioli, S., Ho, M. T., Wiley, D. E. & Pellegrini, L. A. 2018. Thermodynamic modeling of the system of CO2 and potassium taurate solution for simulation of the carbon dioxide capture process. *Chemical Engineering Research and Design,* 136**,** 834-845.

Netl 2010. Cost and Performance Baseline for Fossil Energy Plants Volume 1: Bituminous Coal and Natural Gas to Electricity. *DOE/NETL-2010/1397.*

Netl 2015. Cost and Performance Baseline for Fossil Energy Plants Volume 1a: Bituminous Coal (PC) and Natural Gas to Electricity Revision 3. DOE/NETL-2015/1723

Raksajati, A., Ho, M. T. & Wiley, D. E. 2016. Understanding the Impact of Process Design on the Cost of CO2 Capture for Precipitating Solvent Absorption. *Industrial & Engineering Chemistry Research,* 55**,** 1980-1994.

Raynal, L., Bouillon, P.-A., Gomez, A. & Broutin, P. 2011. From MEA to demixing solvents and future steps, a roadmap for lowering the cost of post-combustion carbon capture. *Chemical Engineering Journal,* 171**,** 742-752.

Sanchez-Fernandez, E. 2013. *Novel Process Designs to Improve the Efficiency of Postombustion Carbon Dioxide Capture.* Technische Universiteit Delft,.

Sanchez-Fernandez, E., De Miguel Mercader, F., Misiak, K., Van Der Ham, L., Linders, M. & Goetheer, E. 2013a. New process concepts for CO 2 capture based on precipitating amino acids. *Energy Procedia,* 37**,** 1160-1171.

Sanchez-Fernandez, E. & Goetheer, E. L. V. 2011. DECAB: Process development of a phase change absorption process. *Energy Procedia,* 4**,** 868-875.

Sanchez-Fernandez, E., Heffernan, K., Van Der Ham, L., Linders, M. J., Brilman, D. W. F., Goetheer, E. L. & Vlugt, T. J. 2014. Analysis of process configurations for CO2 capture by precipitating

amino acid solvents. *Industrial & Engineering Chemistry Research,* 53**,** 2348-2361.

Sanchez-Fernandez, E., Heffernan, K., Van Der Ham, L. V., Linders, M. J., Eggink, E., Schrama, F. N., Brilman, D. W. F., Goetheer, E. L. & Vlugt, T. J. 2013b. Conceptual design of a novel CO2 capture process based on precipitating amino acid solvents. *Industrial & Engineering Chemistry Research,* 52**,** 12223-12235.

Simons, K., Brilman, W., Mengers, H., Nijmeijer, K. & Wessling, M. 2010. Kinetics of CO_2 absorption in aqueous sarcosine salt solutions: influence of concentration, temperature, and CO_2 loading. *Industrial & Engineering Chemistry Research,* 49**,** 9693-9702.

Turton, R., Bailie, R. C., Whiting, W. B. & Shaeiwitz, J. A. 2008. *Analysis, synthesis and design of chemical processes*, Pearson Education.

Vaidya, P. D., Konduru, P., Vaidyanathan, M. & Kenig, E. Y. 2010. Kinetics of carbon dioxide removal by aqueous akaline amino acid salts. *Industrial & Engineering Chemistry Research,* 49**,** 11067-11072.

Van Holst, J., Versteeg, G. F., Brilman, D. W. F. & Hogendoorn, J. A. 2009. Kinetic study of CO_2 with various amino acid salts in aqueous solution. *Chemical Engineering Science,* 64**,** 59-68.

Versteeg, G. F., Kumar, P. S., Hogendoorn, J. A. & Feron, P. H. M. 2003. *Method for absorption of acid gases*.

Wei, C.-C., Puxty, G. & Feron, P. 2014. Amino acid salts for CO 2 capture at flue gas temperatures. *Chemical Engineering Science,* 107**,** 218-226.

Wei, S. C.-C., Puxty, G. & Feron, P. 2013. Amino acid salts for CO2 capture at flue gas temperatures. *Energy Procedia,* 37**,** 485-493.